THEORETICAL ASSESSMENT OF STEADY-STATE MICROBUNCHING (SSMB) FOR PAL-EUV

Youngmin Park[1*], Jaehyun Kim[2], Moses Chung[1,2†],
[1]Pohang University of Science and Technology (POSTECH), Pohang, Republic of Korea
[2]Pohang Accelerator Laboratory, Pohang, Republic of Korea

Abstract

This study presents a theoretical investigation of steady-state microbunching (SSMB) within the design framework of the PAL-EUV ring. An analytic longitudinal dynamics model that includes laser-induced energy modulation, radiation damping and quantum excitation, and nonlinear momentum compaction is formulated to examine whether the baseline ring parameters can support sustained microbunch formation. Using this framework, we evaluate the required energy-chirp strength, the stability conditions for microbucket formation, and the expected radiation power under laser modulation. The analysis further identifies the conditions under which SSMB can be sustained, and provides key guidance for assessing its applicability to the PAL-EUV. These results establish a foundation for subsequent feasibility studies and future experimental development.

INTRODUCTION

Steady-state microbunching (SSMB) is a storage-ring-based light source concept that aims to generate coherent radiation with high repetition rate and high average power. In SSMB, electrons are microbunched at an optical or shorter wavelength scale so that the radiation is enhanced by longitudinal coherence. Since the original proposal, several theoretical and experimental studies have been carried out to investigate SSMB mechanisms, beam dynamics, and possible radiation applications [1–3].

Among the various schemes for generating microbunching in a storage ring, this work focuses on the feasibility of first-turn SSMB in the PAL-EUV ring. In this scheme, an energy modulation induced by an infrared laser is converted into density microbunching after one revolution in a quasi-isochronous storage ring. To satisfy the required longitudinal condition, the PAL-EUV lattice is first corrected by tuning quadrupole and sextupole families. Macroparticle tracking is then performed using ELEGANT [4], and the radiation from the resulting microbunched beam is calculated using SPECTRA [5].

PAL-EUV RING AND ONE-TURN SSMB

PAL-EUV is a compact 400 MeV electron storage ring being developed for EUV radiation applications. The ring has a circumference of 36 m and adopts a 5-bend achromat lattice to achieve low horizontal emittance and high-brightness radiation. The lattice, consisting of 14 quadrupoles and 16 sextupoles per cell, provides sufficient flexibility not only for linear optics correction but also for the control of nonlinear terms.

The low horizontal emittance of PAL-EUV can provide strong transverse coherence in the EUV wavelength range. However, the radiation from a conventional storage-ring beam is not longitudinally coherent, because the bunch length is much longer than the radiation wavelength. To obtain longitudinal coherence, the electron beam must be microbunched at the radiation wavelength or at a related seed-laser wavelength. Among the various schemes for generating microbunching in a storage ring, this study focuses on evaluating the applicability of first-turn SSMB to the PAL-EUV ring. In this scheme, a laser modulator imposes an energy modulation at the laser wavelength, and the modulation is converted into density microbunching after one revolution through the ring.

A stability conditions for first-turn microbunching is that the longitudinal slippage caused by the uncorrelated energy spread should be sufficiently small compared with the laser wavelength. This condition can be written as

$$|\eta| C_0 \sigma_\delta \lesssim \frac{\lambda_L}{2\pi}, \tag{1}$$

Here, η is the slippage factor, C_0 is the ring circumference, σ_δ is the energy spread, and λ_L is the modulation laser wavelength. Since the slippage factor depends on the relative momentum deviation δ, it can be expanded into the leading term η_0 and higher-order terms such as $\eta_1\delta$ and $\eta_2\delta^2$. Therefore, the PAL-EUV lattice should be tuned close to a quasi-isochronous condition while also controlling the nonlinear slippage terms to suppress phase smearing during one-turn transport.

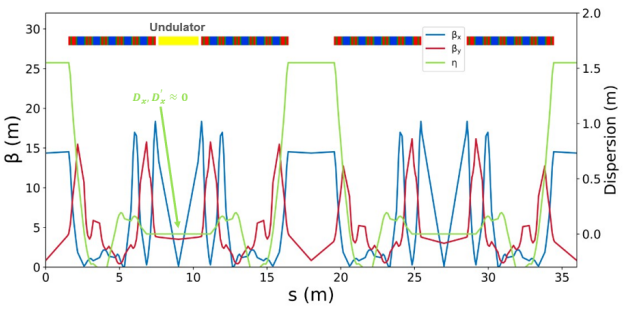

Figure 1: Corrected PAL-EUV lattice and beta functions and horizontal dispersions for the first-turn SSMB study.

* pym102048@postech.ac.kr
† moses@postech.ac.kr

Figure 1 shows the corrected PAL-EUV lattice used for the first-turn SSMB study. For PAL-EUV, $C_0 = 36$ m, $\sigma_\delta = 2.9\times10^{-4}$, and $\lambda_L = 1064$ nm, giving the requirement $|\eta| \lesssim 10^{-5}$. The leading slippage term η_0 was tuned with 14 quadrupole families. The nonlinear slippage terms were corrected using sextupoles. Since the linear chromaticities and the first-order slippage factor are approximately linear with respect to sextupole strength, a response matrix for ξ_x, ξ_y, η_1, and η_2 was constructed from the 16 sextupole families. The four most effective families were selected for correction. The corrected lattice achieved $|\eta_0| \sim 10^{-5}$, $|\eta_1/\eta_0| \sim 10$, and $|\eta_2/\eta_0| \sim 100$.

After setting the slippage factor to satisfy the stability condition, the expected microbunching strength can be evaluated from the analytical bunching factor. For the n-th harmonic and the m-th turn after the laser modulation, the bunching factor is given by

$$|b_{n,m}| = |J_n\left(nk_L m\eta C_0 A\right)| \times \exp\left[-\frac{\left(nk_L m\eta C_0\sigma_\delta\right)^2}{2}\right] \times \exp\left[-\frac{\left(2nk_L\sqrt{\epsilon_x\mathcal{H}_x}|\sin(m\pi\nu_x)|\right)^2}{2}\right]. \quad (2)$$

where J_n is the n-th order Bessel function, k_L is the laser wave number, and A is the normalized laser-induced energy modulation amplitude. The first term in the exponential factor describes the longitudinal smearing caused by the finite energy spread σ_δ through the phase slippage of the ring. The second term represents the additional bunching reduction caused by transverse-longitudinal coupling, which is characterized by the horizontal emittance ϵ_x, the Curly-H function $\mathcal{H}_x$, and the horizontal tune ν_x. Therefore, once the slippage factor is fixed, this expression gives a direct estimate of the expected bunching factor and the corresponding coherent radiation intensity, which scales as $|b_{n,m}|^2$. The effects of modulation amplitude, horizontal emittance, and revolution number on the bunching factor are summarized in Fig. 2.

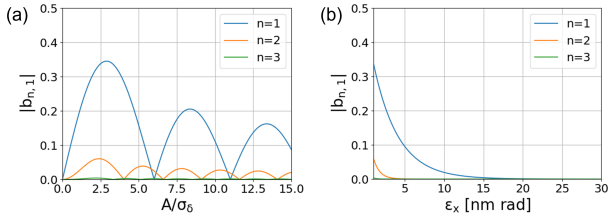

Figure 2: Dependence of the calculated bunching factor on (a) modulation amplitude with $\epsilon_x = 1$ nm, (b) horizontal emittance with $A = 2.5\sigma_\delta$

As shown in Fig. 2, the bunching factor is maximized when the modulation amplitude is approximately $A = 2.5\sigma_\delta$. The laser power required to provide this modulation amplitude can be estimated from the energy modulation induced in the laser modulator,

$$A = \frac{e[JJ]K}{\gamma^2 mc^2}\sqrt{\frac{4P_L Z_0 Z_R}{\lambda_L}}\tan^{-1}\left(\frac{L_u}{2Z_R}\right), \quad (3)$$

where P_L is the modulation laser power, $Z_0 = 376.73\ \Omega$ is the vacuum impedance, Z_R is the Rayleigh length, and L_u is the modulator undulator length. The undulator coupling factor is given by

$$[JJ] = J_0(\chi) - J_1(\chi), \qquad \chi = \frac{K^2}{4+2K^2}. \quad (4)$$

For the present parameters, choosing $Z_R = L_u/3$ gives the required modulation laser power of approximately 4.3 MW to reach $A = 2.5\sigma_\delta$.

TRACKING OF LASER-MODULATED BEAM

To validate the analytical estimates, macroparticle tracking simulations were performed using ELEGANT. First, equilibrium tracking was carried out without laser modulation. A total of 10^4 particles were tracked for 10^5 turns, assuming only an RF cavity with $V_{RF} = 250$ kV and $f_{RF} = 500$ MHz in the storage ring. The resulting equilibrium longitudinal phase-space distribution is shown in Fig. 3. Owing to the low slippage factor of $\eta \simeq 10^{-5}$, a short rms bunch length of approximately 110 fs was obtained, while the rms energy spread was about 4×10^{-4}.

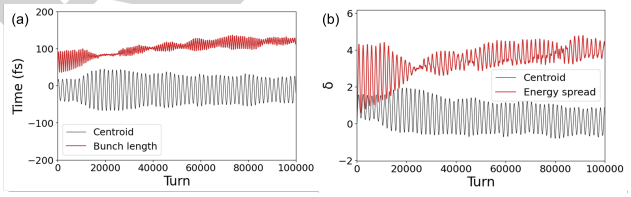

Figure 3: Equilibrium tracking results without laser modulation. (a) Longitudinal centroid and rms bunch length as a function of turn number. (b) Energy centroid and rms energy spread as a function of turn number.

After confirming the equilibrium distribution, one-turn SSMB tracking was performed with 10^5 particles. A sinusoidal energy modulation at $\lambda_L = 1064$ nm was applied to the equilibrium beam. The modulation voltage was set to 400 kV, corresponding to $A = 9.0\times10^{-4}$ for $E_0 = 400$ MeV, or $2.5\sigma_\delta$ for $\sigma_\delta = 3.0\times10^{-4}$. The longitudinal distribution was then observed after one turn.

As shown in Fig. 4, a weak microbunching structure appears near the bunch center after one revolution. The bunching factor was then evaluated from the Fourier component of the longitudinal distribution at the laser wavelength, as shown in Fig. 5, yielding $|b| \simeq 0.12$. This result confirms the formation of microbunching after one revolution under the low-slippage condition.

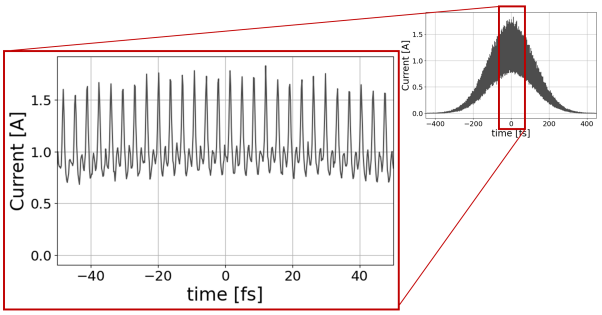

Figure 4: Longitudinal particle distribution after one revolution following the laser modulation. A weak microbunching structure appears near the bunch center under the low-slippage condition.

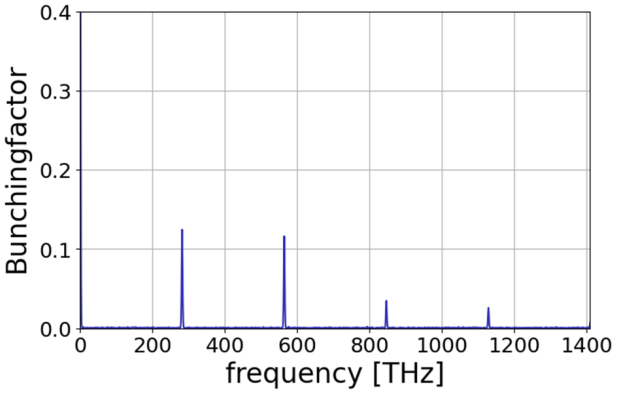

Figure 5: Bunching factor evaluated from the Fourier component of the longitudinal distribution after one revolution. The bunching factor at the laser wavelength is approximately $|b| \simeq 0.12$.

CALCULATION OF COHERENT RADIATION

Finally, the coherent radiation from the microbunched beam was calculated using SPECTRA, as shown in Fig. 6. The calculated FWHM bandwidth is approximately 0.98%, and the peak power is about 100 W. This relatively low power is mainly due to the modest bunching factor obtained from the one-turn tracking simulation. Although the present result demonstrates the formation of microbunching under the corrected low-slippage condition, further optimization is required to enhance the bunching factor and coherent radiation power. In particular, the transverse-longitudinal coupling contribution should be further minimized through the control of the horizontal emittance, Curly-H function, and betatron tune. In addition, the energy-spread growth caused by incoherent synchrotron radiation (ISR) should be included, since it can increase longitudinal smearing and further reduce the bunching factor.

SUMMARY AND OUTLOOK

The feasibility of first-turn SSMB in the PAL-EUV storage ring was studied using lattice optimization, ELEGANT tracking, and SPECTRA radiation calculation. The linear slippage factor was reduced to the order of 10^{-5}, and the nonlinear slippage terms were corrected using sextupoles. Based on the corrected lattice, the analytical bunching-factor estimate was used to evaluate the expected microbunching strength.

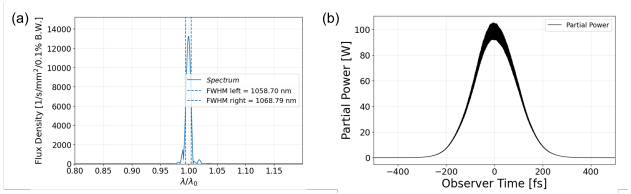

Figure 6: SPECTRA calculation of the coherent radiation from the one-turn microbunched beam: (a) flux density as a function of wavelength and (b) partial power as a function of observer time.

Equilibrium tracking without laser modulation showed that the low-slippage lattice can produce a short bunch with an rms bunch length of approximately 110 fs and an rms energy spread of about 3×10^{-4}. One-turn tracking with a sinusoidal modulation at $\lambda_L = 1064$ nm showed a weak microbunching structure near the bunch center, with a bunching factor of approximately $|b| \simeq 0.12$. The corresponding SPECTRA calculation gave a FWHM bandwidth of 0.98% and a peak power of about 100 W.

The present results demonstrate the basic feasibility of microbunching formation in the corrected low-slippage PAL-EUV lattice. Further improvement requires minimizing the transverse-longitudinal coupling contribution through the control of ϵ_x, $\mathcal{H}_x$, and ν_x. ISR-induced energy-spread growth should also be included in future studies for a more realistic prediction of the achievable bunching factor and radiation power.

REFERENCES

[1] X. Deng, A. Chao, J. Feikes, A. Hoehl, W. Huang, R. Klein, A. Kruschinski, J. Li, A. Matveenko, Y. Petenev, M. Ries, C. Tang, and L. Yan, "Experimental demonstration of the mechanism of steady-state microbunching," Nature, vol. 590, pp. 576–579, 2021. doi:10.1038/s41586-021-03203-0

[2] D. F. Ratner and A. W. Chao, "Steady-State Microbunching in a Storage Ring for Generating Coherent Radiation," *Phys. Rev. Lett.*, vol. 105, p. 154801, 2010. doi:10.1103/PhysRevLett.105.154801

[3] X. Deng, *Theoretical and Experimental Studies on Steady-State Microbunching*, Springer Singapore, 2024.

[4] M. Borland, "Elegant: A flexible SDDS-compliant code for accelerator simulation," Argonne National Lab., IL, USA, Tech. Rep., 2000.

[5] T. Tanaka and H. Kitamura, "SPECTRA: a synchrotron radiation calculation code," *J. Synchrotron Radiat.*, vol. 8, no. 6, pp. 1221–1228, 2001. doi:10.1107/S090904950101425X